

# Impeller Mixing Simulations of Transitional Flow

## Abstract

Impellers have a wide variety of industrial applications and are utilized in many industries. They are an integral part of the mixing process. The potential for operating inefficiencies causing large financial losses motivate the field to develop processes with which to accurately model the mixing process. Computational fluid dynamics (CFD) is a powerful tool for analyzing mixing scenarios. Multiple methodologies were used to simulate impeller mixing at different operating conditions. Results were compared to experimental data provided by SPX Flow to assess the validity of these methodologies. It is hoped that these comparisons will lead to a proper methodology for simulating impellers operating in the transitional flow regime, which has notoriously been a challenging task. Presently, the mixing problem is being evaluated in a baffled tank with an A200 impeller at various Reynolds numbers. Power number and mixing time predictions are calculated and compared with available data and correlations.

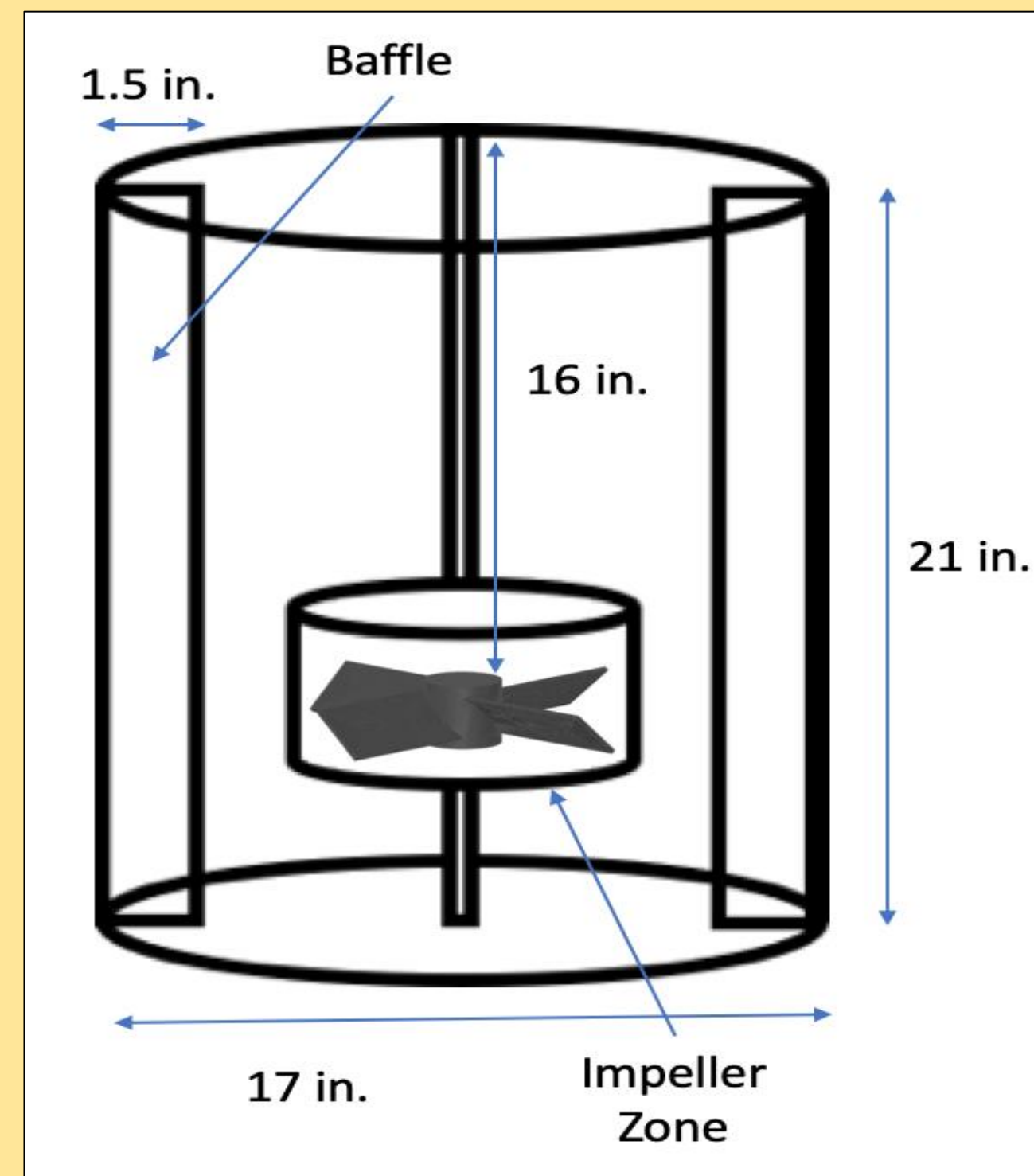


Figure 1: The tank and impeller geometries used in the present simulations. Note the center of the impeller is 16 inches from the top. The impeller diameter is 7 inches.

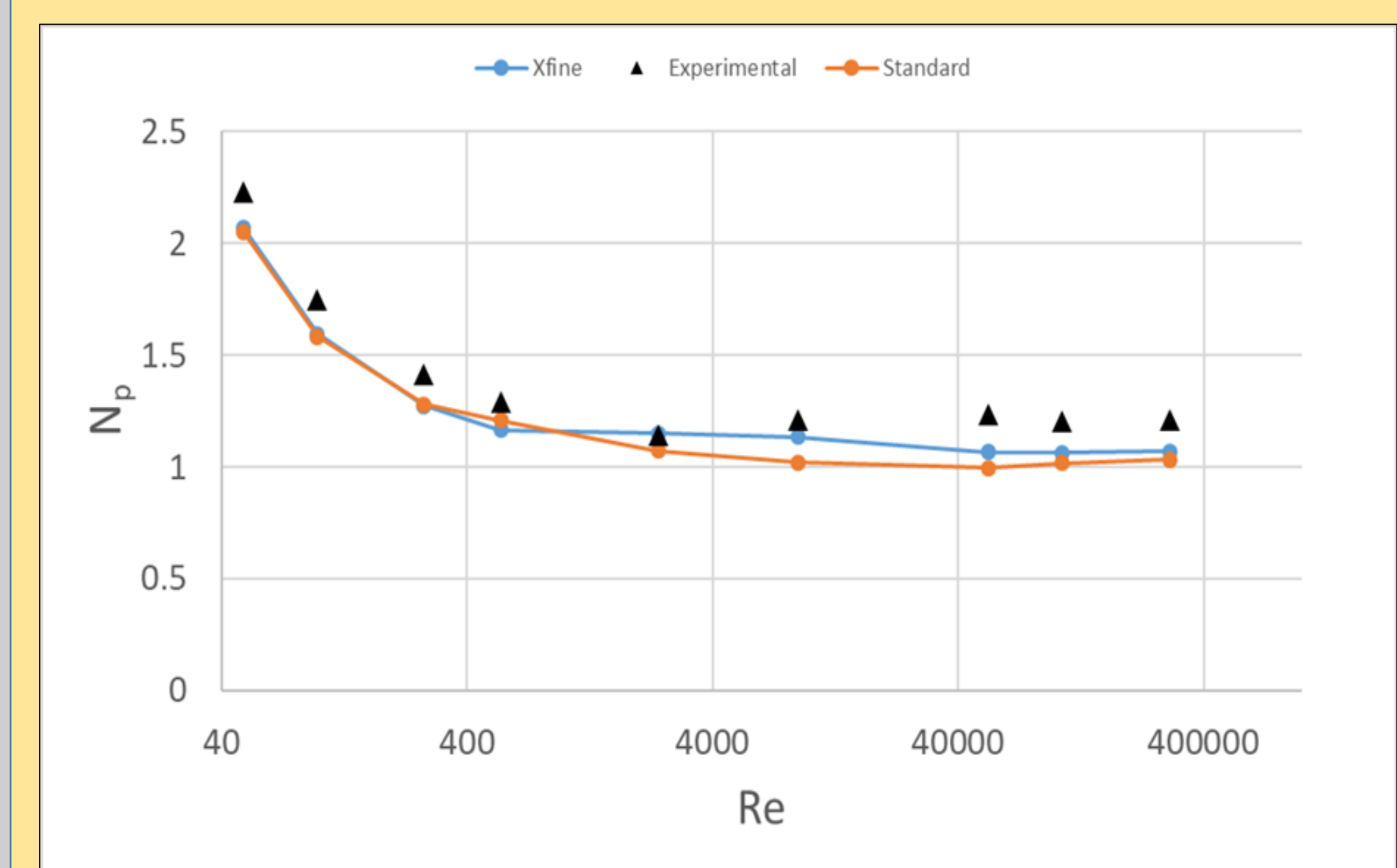


Figure 2: Power number results from simulations that used the standard mesh ("Standard") and the refined impeller mesh ("Xfine"). Results are compared to experimental data for the same system provided by SPX Flow.

## Computational Methodology

Simulations were completed using ANSYS Fluent 18.2. Fluent numerically approximates solutions to the surface/volume integral form of the governing equations for fluid mechanics in a discrete number of "cells". These cells form the entire volume of the tank and together make up a "mesh". Because the fluid solution is assumed constant in each cell, more cells are needed in dynamic regions of the flow field to produce a more accurate solution. For all simulations, Fluent's coupled second-order solver was used, the fluid was assumed to be incompressible and Newtonian, and the realizable  $k-\epsilon$  equations with the Menter-Lechner near wall treatment were solved. Simulations were completed using the supercomputer Bridges, located at the Pittsburgh Supercomputing Center (PSC).

## Impeller Simulations

Simulations were carried out for an A200 impeller in a baffled tank. The tank and impeller geometries are depicted in Figure 1. The tank had four evenly-spaced baffles, and the impeller consisted of four flat blades pitched at a 45° angle, with a diameter of 7 in.

The geometry for the A200 impeller was provided by SPX Flow. Using Autodesk Inventor, the A200 impeller, shown in Figure 1, was placed inside a baffled tank. A multiple reference frame (MRF) simulation was performed to capture both the rotation of the impeller and the fixed tank and baffles. See Ref. [1] for more information. Following the MRF approach, the fluid region of the mixing system was split into two zones. The "tank zone" included the fixed tank walls and baffles but stopped at the cylindrical zone in the middle. The "impeller zone" was contained in the cylinder inside the tank zone and included the impeller geometry. These two zones are pictured in Figure 1. In the MRF simulation, the impeller zone was set to a rotational reference frame, while the tank zone was stationary. This was done to simulate the spinning of the impeller blade. The MRF model assumes that the flow near the impeller and the flow near the baffles are de-coupled, so that a fully-rotating impeller simulation is not required.

The boundary conditions used in our simulations are as follows. First, the walls and impeller surfaces utilized the no-slip condition. Second, the top surface was prescribed to be a wall with zero wall shear stress. This was used to simulate a scenario in which there was no wall at the top of the tank and the fluid at the top was perfectly flat.

Once a surface mesh was formed for the given geometry, the volume mesh was calculated using Fluent Meshing's "auto mesh" feature. Within the auto mesh settings, a zone-specific prism layer was created around the impeller. The volume fill was set to use the hexcore method. Additionally, refinement regions were used to increase the number of cells around specific features. Refinement regions were added to the bottom of the tank and around the baffles. The standard mesh for the cases described here contained  $2.3 \times 10^6$  cells.

## Results

Several quantities are important when discussing impeller mixing scenarios: the Reynolds number, the power number, and the mixing time. The Reynolds number is defined as  $Re = \rho ND^2 / \mu$ , where  $\rho$  is the fluid density,  $N$  is the impeller rotation rate in revolutions per second,  $D$  is the diameter of the impeller, and  $\mu$  is the fluid viscosity. The Reynolds number is a non-dimensionalized input for the simulation which describes the operational state of the impeller and tank system. There are three regimes of fluid flow that can be described by the Reynolds number: laminar, transitional, and turbulent. Laminar ranges from approximately  $Re = 0$  to 20 and is characterized by smooth flow with little time dependence. The turbulent range is above  $Re = 2000$  and has chaotic time-dependent flow. The transitional flow regime occurs approximately from  $Re = 20 - 2000$ , and the flow is characterized as being neither distinctly laminar or turbulent [2].

A second important quantity, the power number, is given by  $N_p = 2\pi\tau / \rho N^2 D^5$ , where  $\tau$  is the torque required to spin the impeller [1]. The power number is a non-dimensionalized output of the simulation which represents the power required to turn the impeller. Power number predictions are shown for the standard mesh in Figure 2. To ensure converged power number predictions, an additional simulation was completed using a refined impeller mesh with a Global Max Length of 0.125". Results are also shown in Figure 2. When compared to the standard mesh, the refined impeller mesh generated very similar power number results, and both simulations under-predicted the corresponding experimental data.

A third important quantity is the mixing time. In order to predict mixing time as a function of the Reynolds number, time-dependent passive scalar simulations were performed based on the previously computed steady-state MRF flow field results. See Refs. [3] and [4] for more information. The amount of time to mix,  $\theta_{95}$ , was defined as the time required for the concentration of an injected passive scalar to come within  $\pm 5\%$  of the calculated homogeneous value at the last of three measurement locations. These locations are shown in Figure 3. To initialize the simulations, two separate passive scalars were initialized to a value of 1 inside two spheres and set to 0 elsewhere. In order to assess the accuracy of the present mixing time predictions, they were compared to expected empirical mixing time correlations for laminar, transitional, and turbulent flow regimes using the non-dimensional form of mixing time,  $N\theta_{95}$  [1]. The mixing times as a function of the Reynolds number were predicted within 50% in the turbulent regime, as shown in Figure 4. Additionally, the general trend of increasing mixing time as the Reynolds number decreases matches the empirical correlation. However, mixing time values clearly diverged from experimental correlation in the laminar and transitional flow regions.

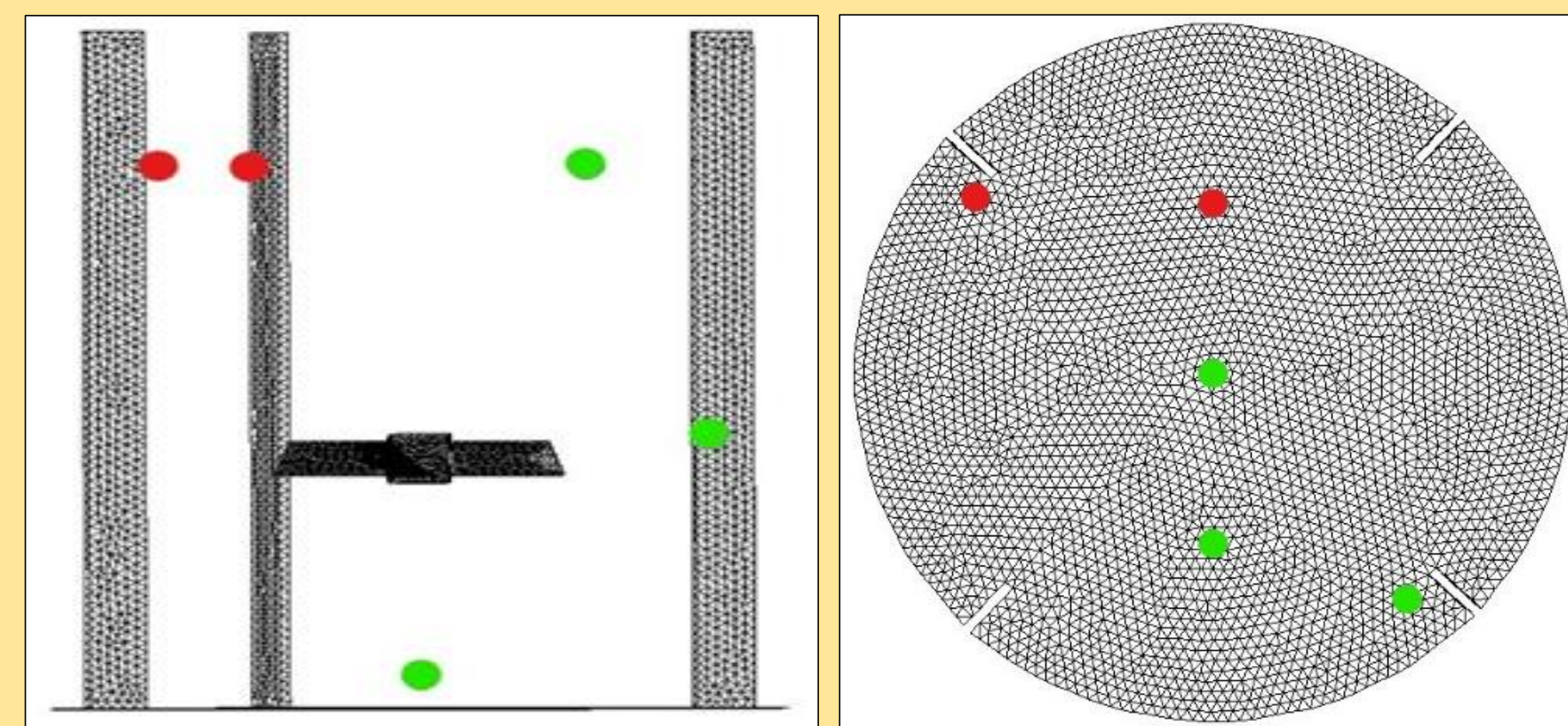


Figure 3: Two passive scalar injection sites (red) were used for predicting the mixing time. Concentration as a function of time was measured at three probe point locations (green). The left image provides a side view of the tank-impeller system and the right image is viewed from above.

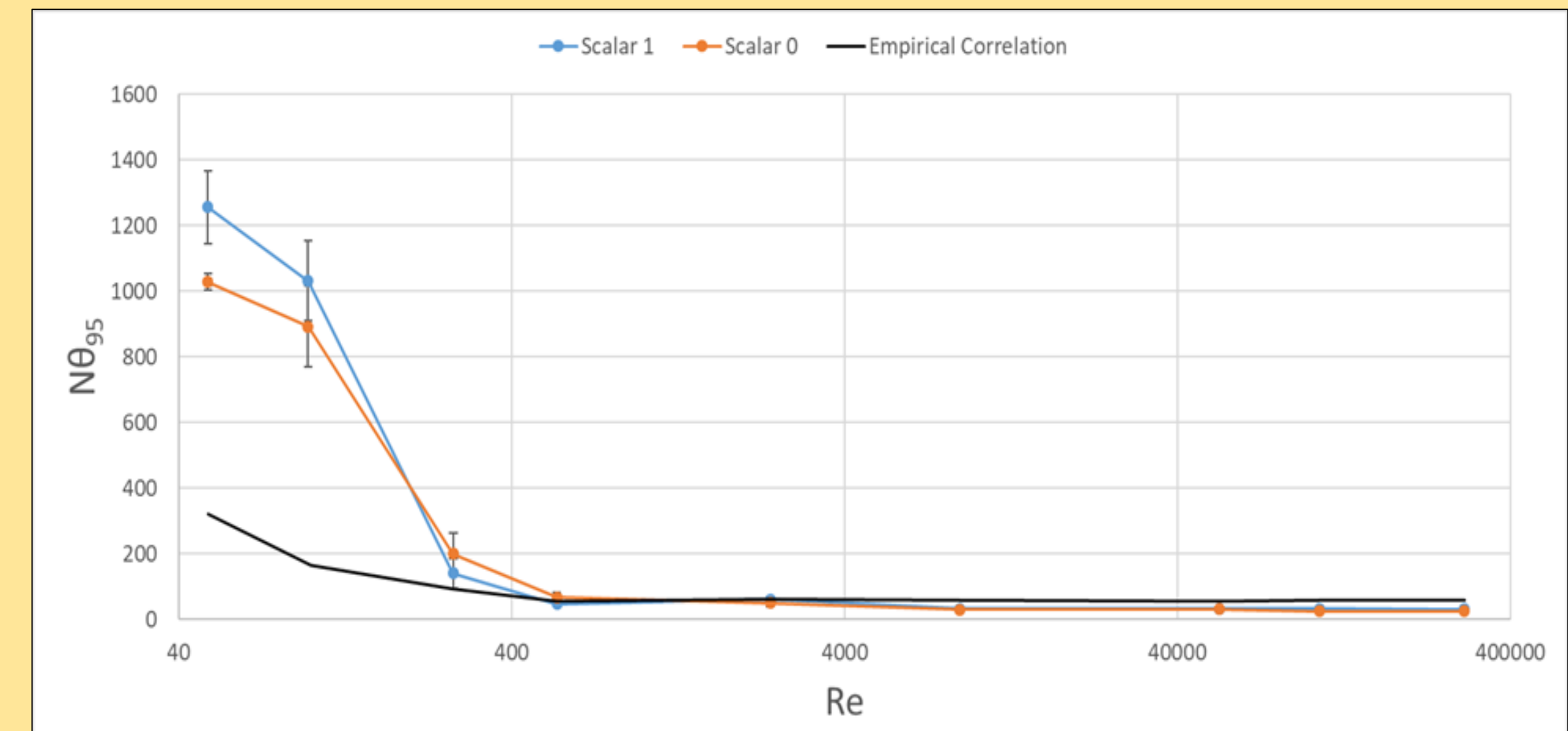


Figure 4: Non-dimensionalized mixing time as a function of the Reynolds number. Scalar 0 was initialized above the impeller away from the tank wall. Scalar 1 was initialized above the impeller in front of the baffle. Both scalar injection sites can be seen in Figure 3. Empirical correlations for laminar, transitional, and turbulent flow mixing (taken from Ref. [1]) are also plotted for comparison.

## Conclusions

Simulations for impeller mixing have a wide variety of applications, but must be tuned to produce meaningful results. The results obtained using extra grid refinement here still under-predicted the values for the experimental power numbers, and showed no significant differences when compared to the previous cases with less refinement, suggesting that our baseline mesh is likely a reasonable choice for future simulations. Time-dependent passive scalar simulations were also performed to predict the mixing time required for the impeller system as a function of the Reynolds number. In predicting mixing time, nondimensionalized mixing times were compared to empirical correlations for laminar, transitional, and turbulent flow mixing. Overall, the trend of  $N\theta_{95}$  as a function of the Reynolds number was predicted well, and simulations in the turbulent regime were the most accurate. However, mixing time was predicted less accurately in the laminar and transitional regimes. To obtain better agreement with the empirical correlations, it may be necessary to perform unsteady simulations of the flow field using a sliding mesh to better capture the time-dependent nature of transitional flow. Also, the effect of certain simulation settings, such as the Schmidt number, should be explored. It is also critical that we obtain experimental data in all flow regimes to allow for more accurate testing of our simulation results.

## Acknowledgements

The authors would like to thank Dr. David Foster from the University of Rochester for collaborating with us on this project. We would also like to thank SPX Flow for providing the experimental data as well as the A200 impeller geometry file. The present work would not have been possible without both of these contributors. Additionally, we would like to express our gratitude to XSEDE for providing us access to PSC Bridges in order to complete simulations. Similarly, we are grateful to Houghton College and the Summer Research Institute for providing the opportunity and workspace to conduct the present work.

## References

- [1] *Handbook of Industrial Mixing: Science and Practice*, edited by E.L. Paul, V.A. Atiemo-Obeng, S.M. Kresta (John Wiley & Sons, Inc., 2004).
- [2] R.J. Weetman, in *Fluid Mechanics of Mixing: Modelling, Operations and Experimental Techniques*, edited by R. King (Springer Science+Business Media Dordrecht, 1992). pp. 19-26.
- [3] O. Zikanov. *Essential Computational Fluid Dynamics*, 1<sup>st</sup> ed. (John Wiley & Sons, Incorporated, 2011), pp. 11-20.
- [4] G. Montante, M. Moštek, M. Jahoda, F. Magelli, "CFD simulations and experimental validation of homogenisation curves and mixing time in stirred Newtonian and pseudoplastic liquids", *Chemical Engineering Science*, 60 (8-9), 2005, pp. 2427-2437.